Electronic Supplementary Information

Stepwise Observation and Quantification and Mixed Matrix Membrane Separation of CO_2 within a Hydroxyl-Decorated Porous Host

Christopher G. Morris,[1,2] Nicholas M. Jacques,[1] Harry G. W. Godfrey,[1] Tamoghna Mitra,[3] Detlev Fritsch,[4] Zhenzhong Lu,[1] Claire A. Murray,[2] Jonathan Potter,[2] Tom M. Cobb,[2] Fajin Yuan,[2] Chiu C. Tang[2]*, Sihai Yang[1]* and Martin Schröder[1]*

1. School of Chemistry, University of Manchester, Oxford Road, Manchester, M13 9PL, UK. Sihai.Yang@manchester.ac.uk; M.Schroder@manchester.ac.uk

2. Diamond Light Source, Harwell Science and Innovation Campus, Didcot, Oxfordshire, OX11 0DE, UK. chiu.tang@diamond.ac.uk

3. Department of Chemistry, University of Liverpool, Liverpool, L69 7ZD, UK.

4. Fraunhofer IAP, FB3, Geiselbergstrasse 69, Potsdam-Golm, 14476, Germany.

ESI Index

1. Gas Panel

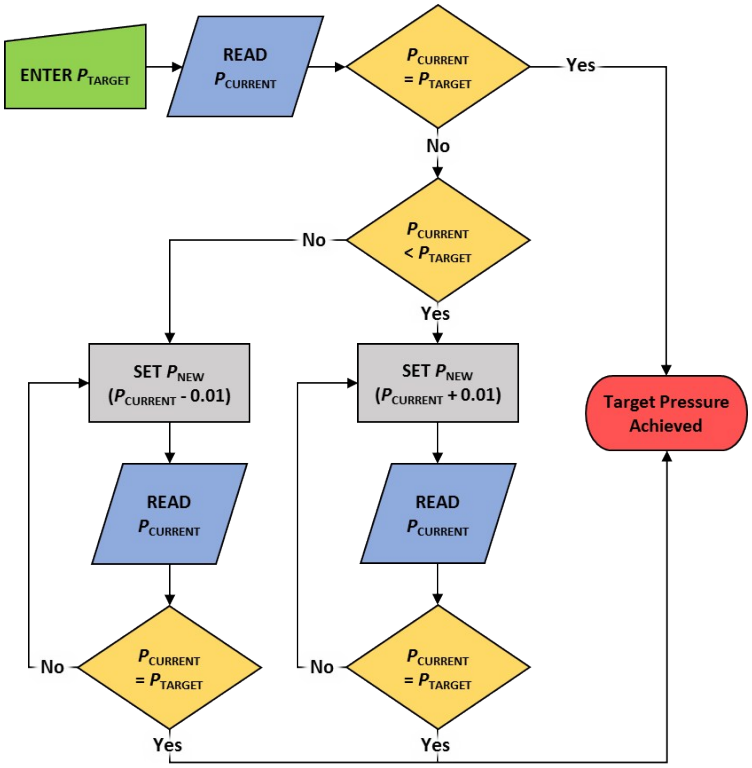

Figure S1. Flow diagram of the logic used for sample dosing. The loops ensure control of gradual incremental pressure.

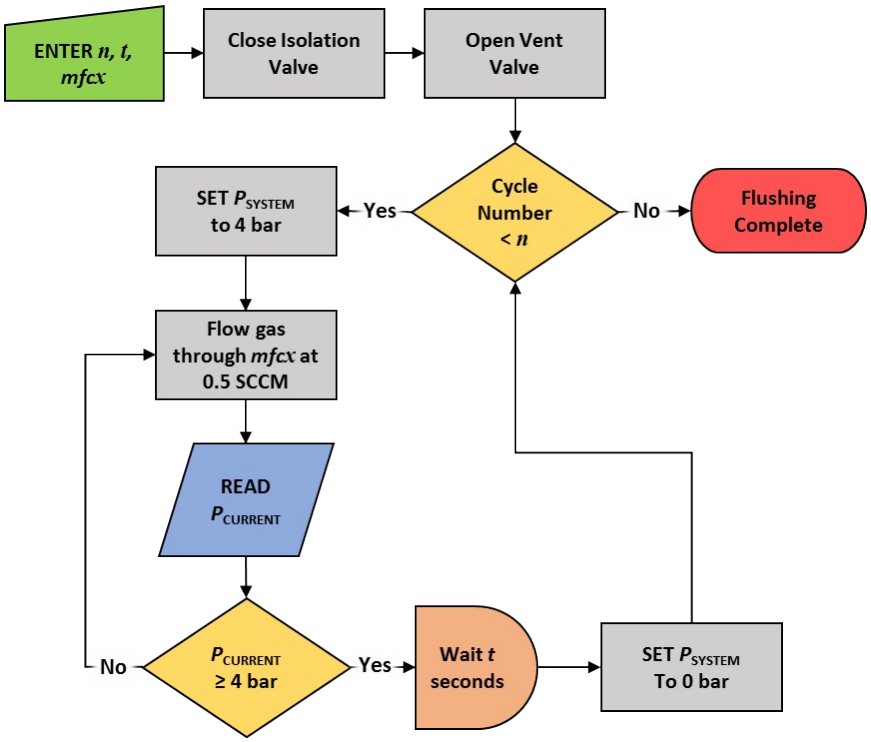

Figure S2. Flow diagram of the logic used for flushing the system.

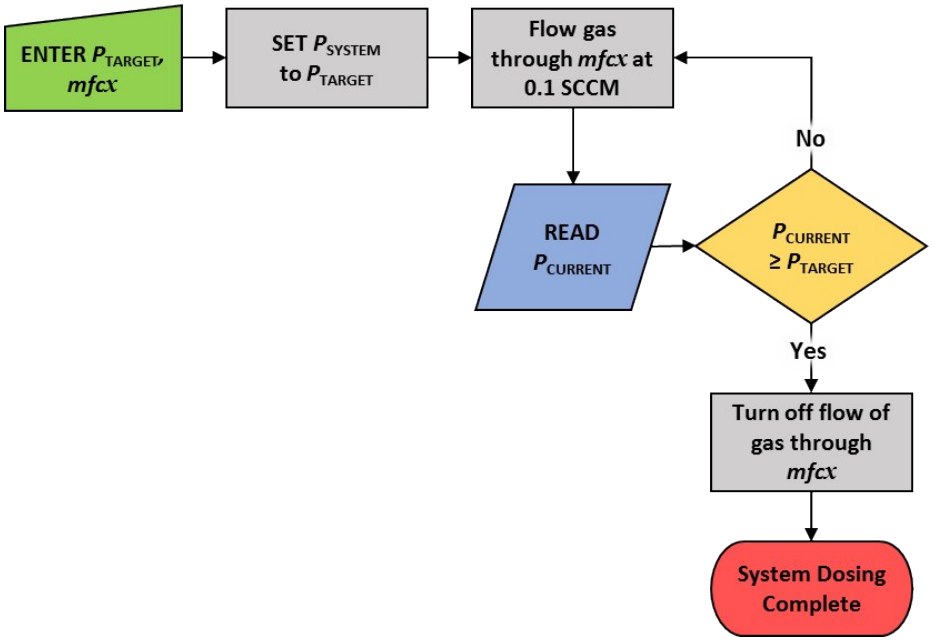

Figure S3. Flow diagram of the logic used for dosing the system.

2. Unit Cell Analysis

Plots of *a* and *c* parameters derived from the Pawley refinements of the single component CO_2 experiments as a function of pressure are shown in Figure S4. A general decrease in length is observed for each parameter. From the structural refinements, this trend can be explained by the μ-OH---O=C=O and the two O=C=O---C(=O)$_2$ interactions forming a network of interactions that generate an increase in 'attractive' force within the pore, and this causes the framework to contract along both axes. Conversely, lattice parameters obtained from the dual component experiments show a general increase in length of the *a* and *c* parameters with increasing pressure (Figure S5), likely due to the presence of disordered non-interacting N_2 inside the pore causing the channel to expand as a result of repulsion. This is supported by the fact that expansion along the *a* axis, an axis very much dependent on the pore width, is much greater than expansion along the *c* axis.

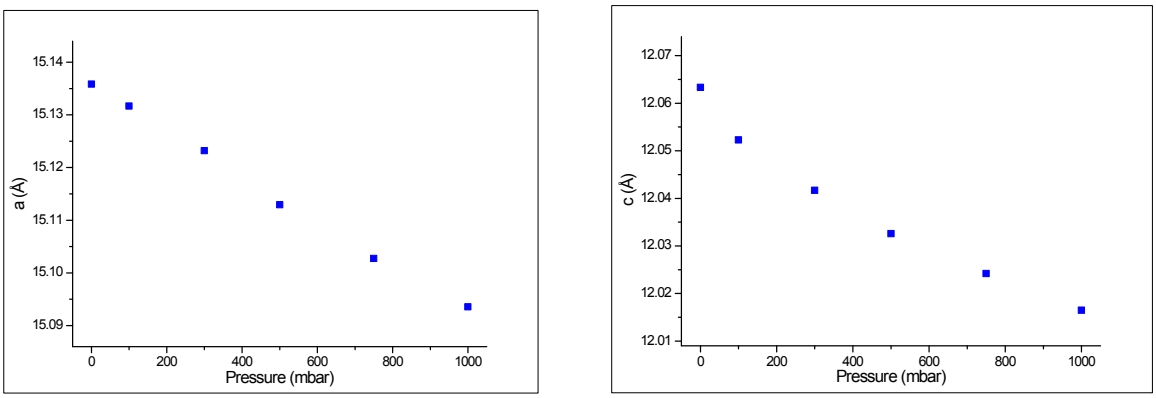

Figure S4. Left: Plot of parameter *a* vs. pressure from the single component CO_2 adsorption experiment. Right: Plot of parameter *c* vs. pressure from single component CO_2 adsorption experiment.

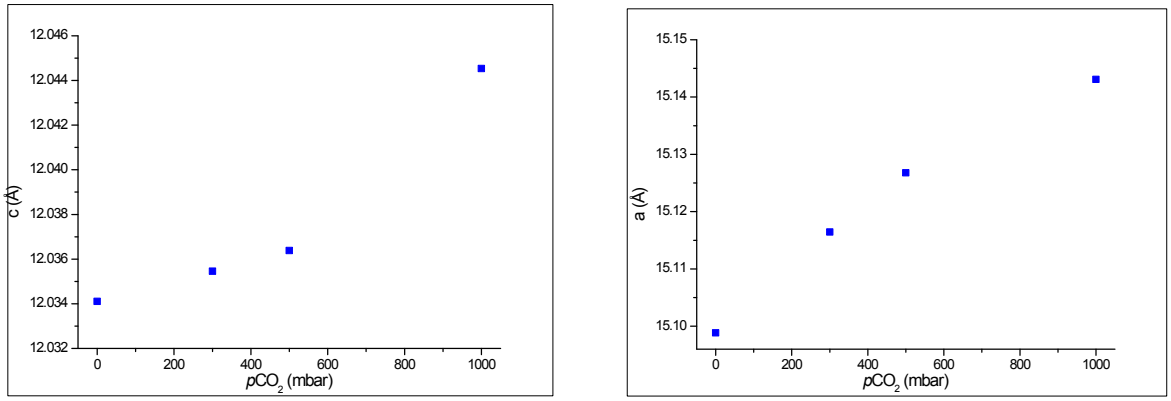

Figure S5. Left. Plot of parameter *a* vs. pressure from dual component N_2/CO_2 adsorption experiment. Right: Plot of *c* parameter vs. pressure from dual component N_2/CO_2 adsorption experiment.

3. Rietveld refinement details

Pressure (mbar)	*a* (Å)	*c* (Å)	Volume (Å^3)	R_{wp}	GOF
0	15.13549(4)	12.06324(4)	2763.48(2)	9.538	2.550
100	15.13178(3)	12.05232(3)	2759.63(1)	6.850	1.803
300	15.12359(4)	12.04198(3)	2754.28(2)	6.684	1.758
500	15.11334(4)	12.03274(4)	2748.43(2)	6.613	1.735
750	15.10345(4)	12.02468(4)	2743.00(2)	6.392	1.677
1000	15.09548(5)	12.01748(5)	2738.47(2)	6.647	1.745
ppCO_2 (mbar)	*a* (Å)	*c* (Å)	Volume (Å^3)	R_{wp}	GOF
300	15.116456(86)	12.0355(1)	2750.190(4)	7.369	2.070
500	15.126742(89)	12.0363(1)	2754.12(4)	7.602	2.176
1000	15.142282(62)	12.04491(6)	2761.76(3)	9.031	2.592

Table S1. Unit cell and Rietveld refinement results from single component CO_2 adsorption experiment

Table S2. Unit cell and Rietveld refinement results from equimolar CO_2/N_2 adsorption experiment

Fits of Rietveld refinements from single component CO_2 adsorption experiments

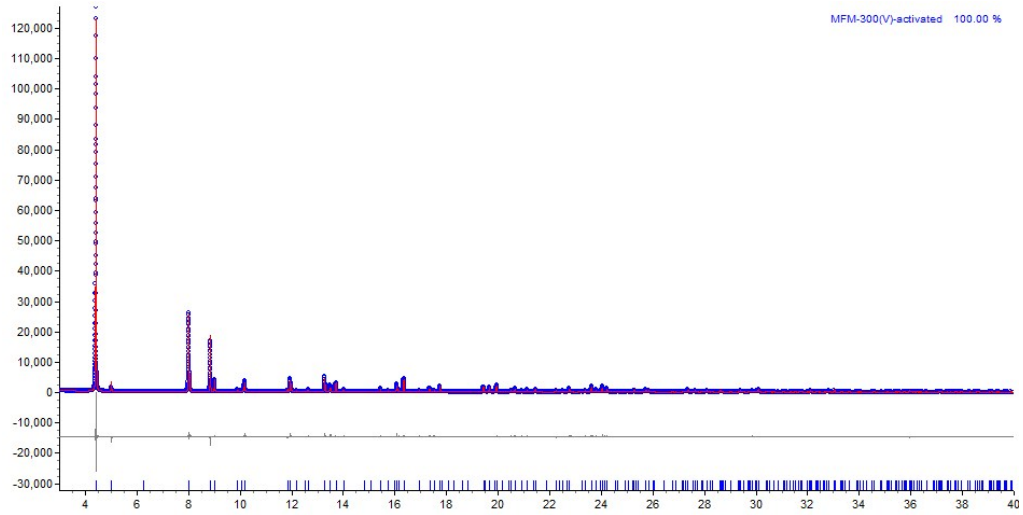

Figure S6. Rietveld refinement plot of MFM-300(V^{III}). Blue open circle = observed; red line = calculated; grey line = difference.

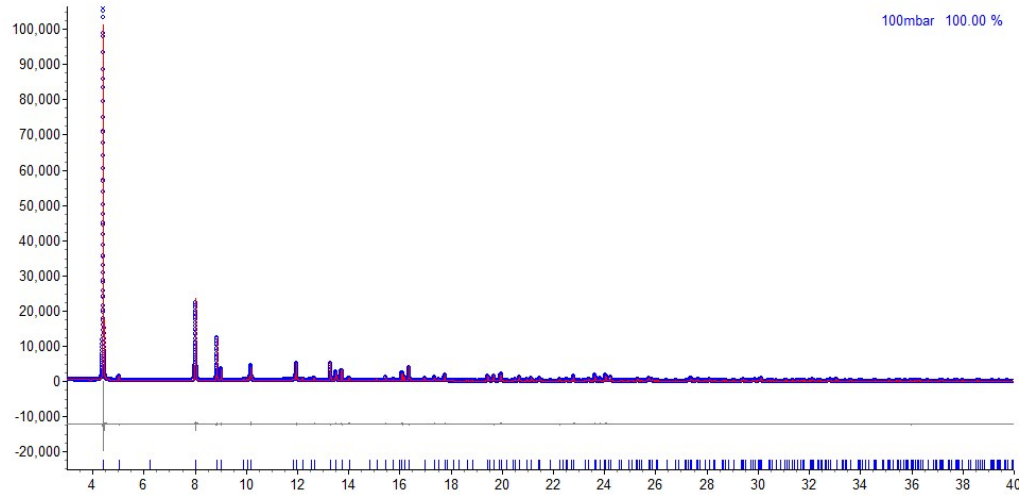

Figure S7. Rietveld refinement plot of MFM-300(V^{III})-I. Blue open circle = observed; red line = calculated; grey line = difference.

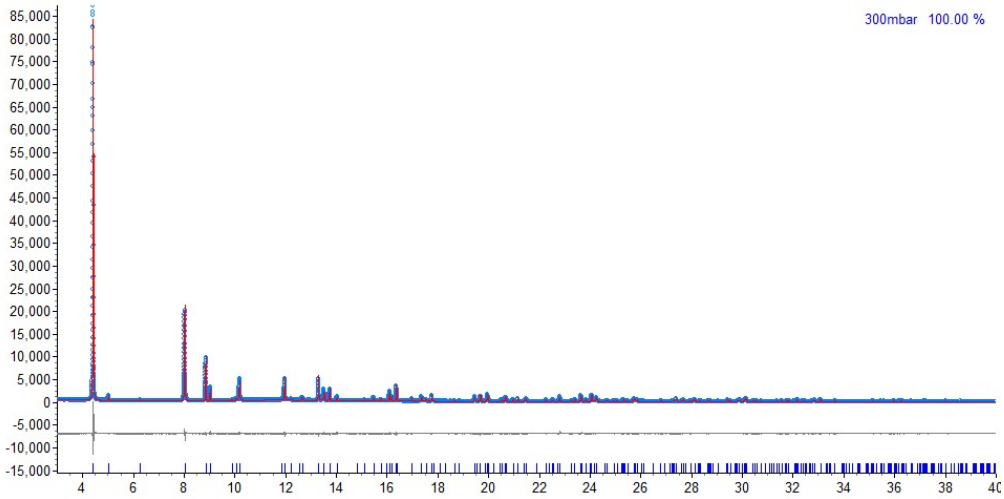

Figure S8. Rietveld refinement plot of MFM-300(V^{III})-II. Blue open circle = observed; red line = calculated; grey line = difference.

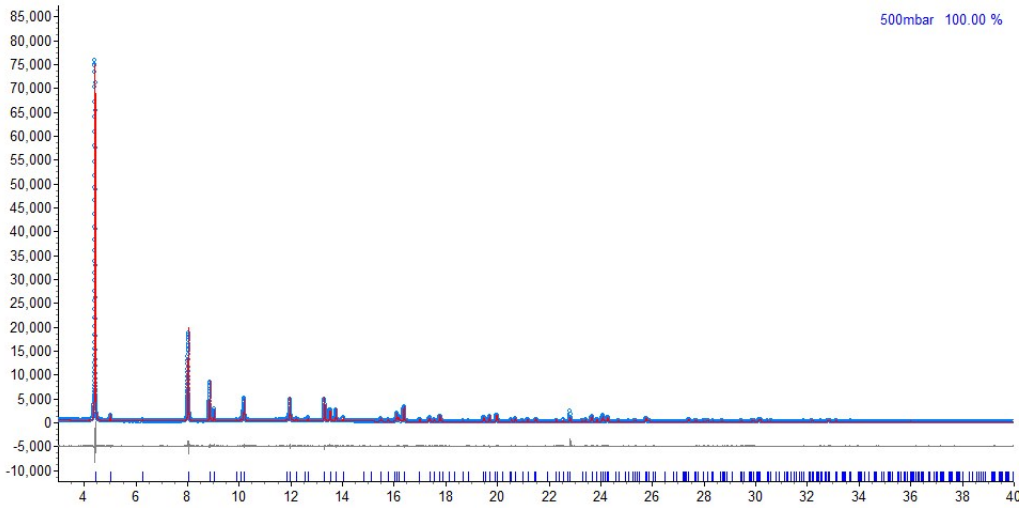

Figure S9. Rietveld refinement plot of MFM-300(V^{III})-III. Blue open circle = observed; red line = calculated; grey line = difference.

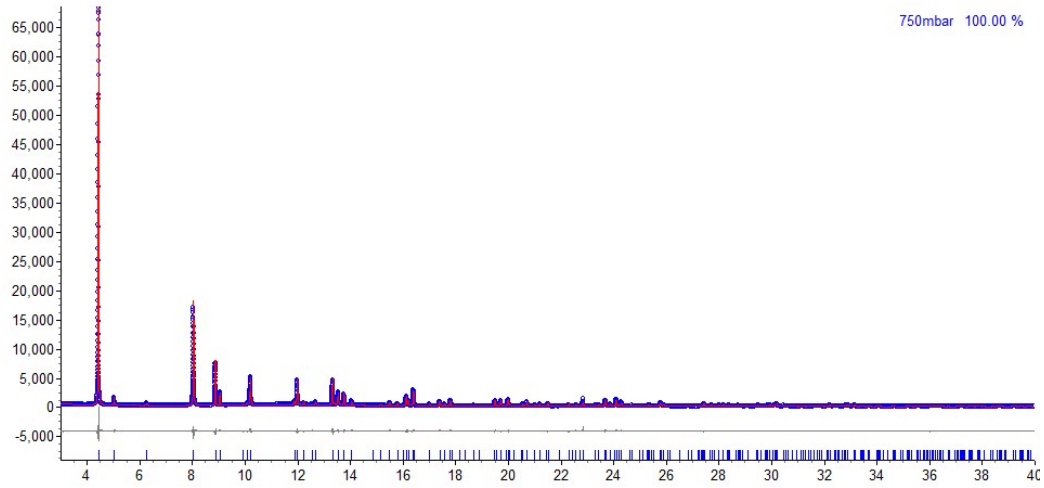

Figure S10. Rietveld refinement plot of MFM-300(V^{III})-IV. Blue open circle = observed; red line = calculated; grey line = difference.

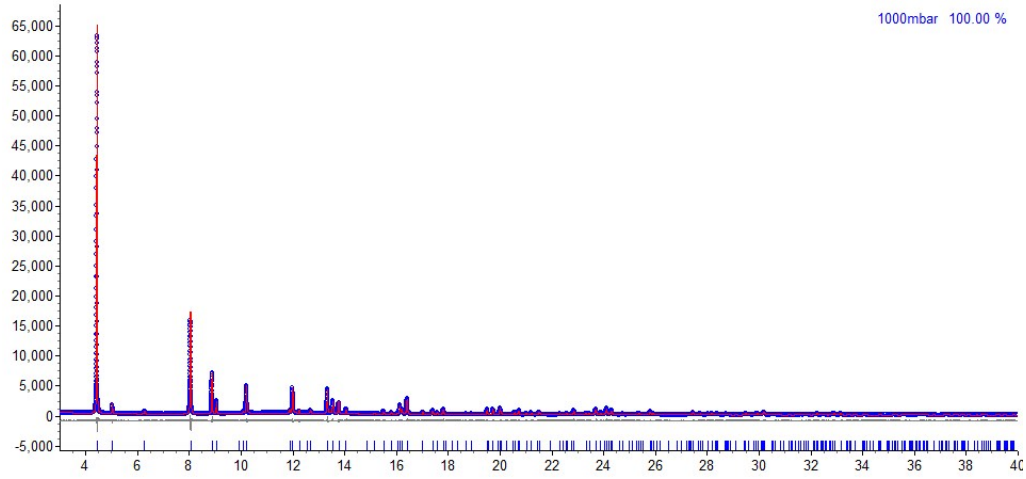

Figure S11. Rietveld refinement plot of MFM-300(V^{III})-V. Blue open circle = observed; red line = calculated; grey line = difference.

Fits of Rietveld refinements from dual component N_2/CO_2 adsorption experiment

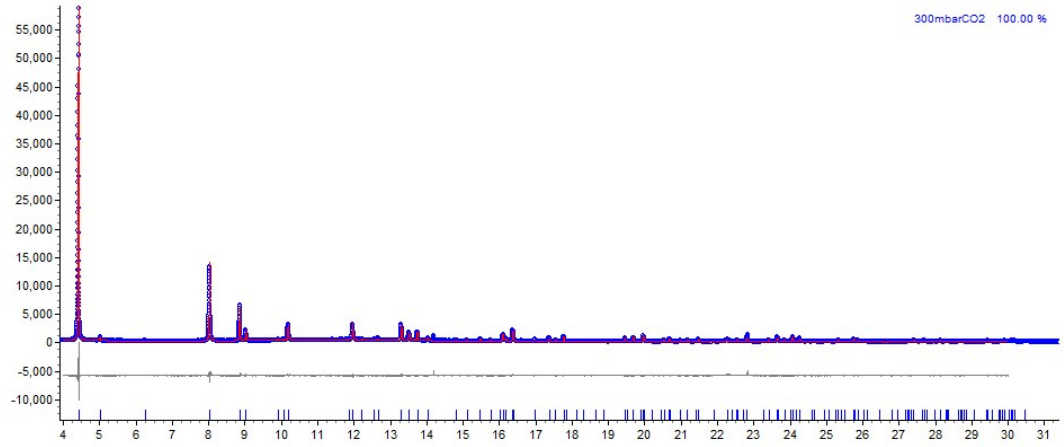

Figure S12. Rietveld refinement plot of MFM-300(V^{III})-VI. Blue open circle = observed; red line = calculated; grey line = difference.

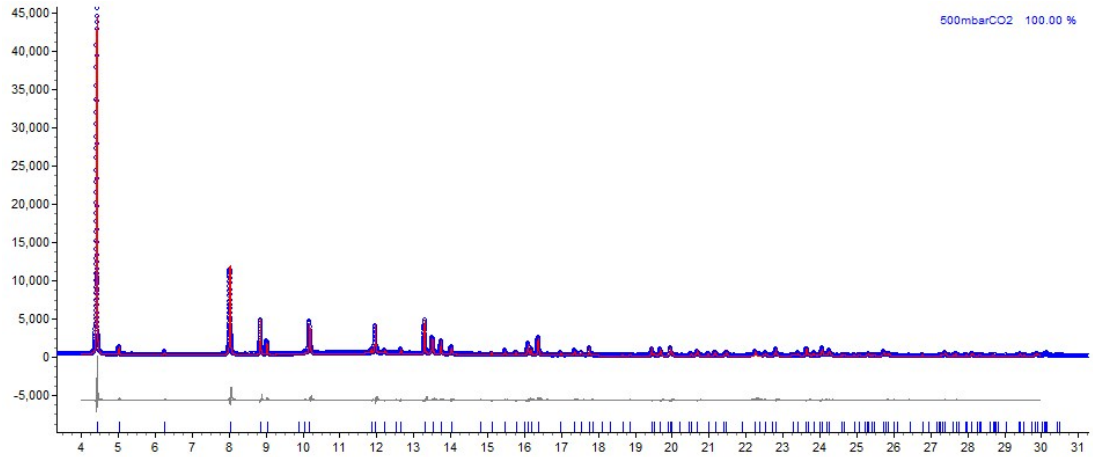

Figure S13. Rietveld refinement plot of MFM-300(V^{III})-VII. Blue open circle = observed; red line = calculated; grey line = difference.

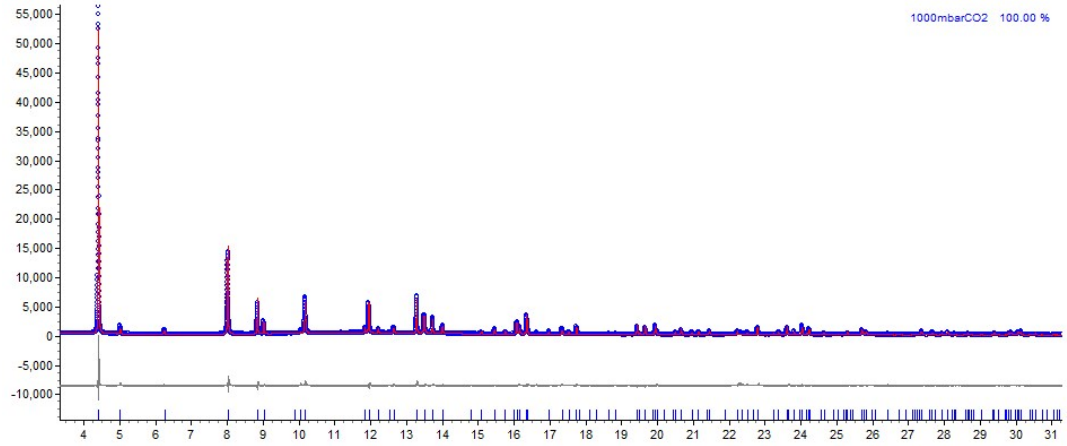

Figure S14. Rietveld refinement plot of MFM-300(V^{III})-VII. Blue open circle = observed; red line = calculated; grey line = difference.

4. Calculation of Adsorption Selectivity of CO_2/N_2

The CO_2 and N_2 sorption data for MFM-300(V^{III}) measured at 273 K were fitted by the virial equation (1).

$$\ln(P) = \ln(Va)+(a0+a1*Va+a2*Va^2 \ldots + a6*Va^6)/T+(b0+b1*Va) \quad (1)$$

where ***P*** is pressure, ***Va*** is amount adsorbed, ***T*** is temperature, and **a0**, **a1**, **a2** … ,**a6** and **b0**, **b1** are temperature independent empirical parameters.

Henry's constant (***KH***) is calculated from equation (2), where ***T*** is temperature.

$$KH = \exp(-b0)\cdot\exp(-a0/T) \quad (2)$$

The Henry's Law selectivity (S_{ij}) for gas *i* over *j* at 273K and 298 K is calculated from the following equation (3).

$$S_{ij} = K_{Hi}/K_{Hj} \quad (3)$$

Virial fitting results and Henry's constants K_H for CO_2 and N_2 in MFM-300(V^{III}) from isotherm data at 273 K

	CO_2	N_2
KH (mol g^{-1} bar^{-1})	27.5	0.339
Fitting R^2	>0.999	0.993
CO_2/N_2 Selectivity	81	

5. Atomic Coordinates

Atomic Coordinates for activated MFM-300(V^{III})

Site	*x*	*y*	*z*	Occupancy	B_{iso} (Å^2)
V	0.68986(7)	0.31014(7)	0.5	1	1.00(3)
O1	0.7443(3)	0.25	0.625	1	1.01(5)
O2	0.89717(19)	0.29233(19)	0.9829(2)	1	1.01(5)
O3	0.6189(2)	0.3729(2)	0.3826(2)	1	1.01(5)
C1	0.5919(3)	0.3589(3)	0.7108(4)	1	1.63(7)
C2	0.5414(3)	0.4319(3)	0.7632(4)	1	1.63(7)
C3	0.5	0.5	0.7080(5)	1	1.63(7)
C4	0.5456(3)	0.4327(3)	0.8818(3)	1	1.63(7)
C5	0.5	0.5	0.9372(4)	1	1.63(7)
H3	0.5	0.5	0.631(3)	1	1.96(8)
H4	0.57318	0.38162	0.90735	1	1.96(8)
H1	0.806	0.25	0.625	1	1.96(8)

Atomic Coordinates for MFM-300(V)-100mbarCO_2

Site	*x*	*y*	*z*	Occupancy	B_{iso} (Å^2)
V	0.690570(50)	0.309430(50)	0.5	1	3.749(24)
O1	0.74830(21)	0.25	0.625	1	3.704(39)
O2	0.89895(15)	0.28981(14)	0.99186(21)	1	3.704(39)
O3	0.62028(16)	0.38135(16)	0.39090(17)	1	3.704(39)
C1	0.59304(29)	0.36025(24)	0.70179(29)	1	4.617(59)
C2	0.54000(25)	0.43078(26)	0.75990(36)	1	4.617(59)
C3	0.5	0.5	0.70384(39)	1	4.617(59)
C4	0.54135(26)	0.42957(25)	0.87919(26)	1	4.617(59)
C5	0.5	0.5	0.93588(31)	1	4.617(59)

H3	0.5	0.5	0.6267(31)	1	5.541(71)
H4	0.57318	0.38162	0.90735	1	5.541(71)
H1	0.806	0.25	0.625	1	5.541(71)
C6	0.7595(20)	0.5376(18)	0.9408(18)	0.3335(35)	15.81(55)
O4	0.74263(99)	0.46332(72)	0.9319(11)	0.3335(35)	15.81(55)
O5	0.7765(11)	0.6116(11)	0.9480(15)	0.3335(35)	15.81(55)
C7	0.8943(64)	0.7945(69)	-0.0750(61)	0.1084(32)	17.3(14)
O6	0.8774(37)	0.7522(37)	-0.1539(60)	0.1084(32)	17.3(14)
O7	0.8951(29)	0.8288(26)	0.0123(59)	0.1084(32)	17.3(14)

Atomic Coordinates for MFM-300(V)-300mbarCO_2

Site	*x*	*y*	*z*	Occupancy	B_{iso} (Å^2)
V	0.690800(48)	0.309200(48)	0.5	1	3.550(25)
O1	0.74625(22)	0.25	0.625	1	3.632(40)
O2	0.89849(15)	0.28984(13)	0.99324(22)	1	3.632(40)
O3	0.62073(17)	0.38260(16)	0.39037(16)	1	3.632(40)
C1	0.59003(29)	0.36026(24)	0.70240(30)	1	4.538(58)
C2	0.54299(25)	0.43307(26)	0.76040(40)	1	4.538(58)
C3	0.5	0.5	0.70380(40)	1	4.538(58)
C4	0.54626(29)	0.43256(27)	0.87937(27)	1	4.538(58)
C5	0.5	0.5	0.93619(32)	1	4.538(58)
H3	0.5	0.5	0.6266(31)	1	5.446(69)
H4	0.57318	0.38162	0.90735	1	5.446(69)
H1	0.806	0.25	0.625	1	5.446(69)
C6	0.7595(20)	0.5376(20)	0.9408(19)	0.4194(50)	20.45(61)
O4	0.74263(93)	0.46332(66)	0.9319(12)	0.4194(50)	20.45(61)
O5	0.7765(11)	0.6116(13)	0.9480(17)	0.4194(50)	20.45(61)

C7	0.8976(56)	0.7904(55)	-0.0751(39)	0.2793(49)	32.7(12)
O6	0.8841(32)	0.7497(26)	-0.1560(47)	0.2793(49)	32.7(12)
O7	0.9007(23)	0.8301(18)	0.0087(42)	0.2793(49)	32.7(12)

Atomic Coordinates for MFM-300(V)-500mbarCO_2

Site	*x*	*y*	*z*	Occupancy	B_{iso} (Å^2)
V	0.691230(50)	0.308770(50)	0.5	1	3.825(26)
O1	0.74470(22)	0.25	0.625	1	3.740(41)
O2	0.89912(15)	0.28965(14)	0.99401(24)	1	3.740(41)
O3	0.62005(17)	0.38197(16)	0.39104(17)	1	3.740(41)
C1	0.59123(29)	0.36045(25)	0.70242(31)	1	4.783(60)
C2	0.54327(26)	0.43316(27)	0.76017(42)	1	4.783(60)
C3	0.5	0.5	0.70333(42)	1	4.783(60)
C4	0.54678(30)	0.43276(28)	0.87918(28)	1	4.783(60)
C5	0.5	0.5	0.93620(33)	1	4.783(60)

H3	0.5	0.5	0.6260(32)	1	5.740(72)
H4	0.57318	0.38162	0.90735	1	5.740(72)
H1	0.806	0.25	0.625	1	5.740(72)
C6	0.7595(17)	0.5376(19)	0.9408(17)	0.4345(51)	18.54(53)
O4	0.74263(83)	0.46332(62)	0.9319(11)	0.4345(51)	18.54(53)
O5	0.77654(97)	0.6116(12)	0.9480(15)	0.4345(51)	18.54(53)
C7	0.8976(58)	0.7904(53)	-0.0751(35)	0.3506(53)	37.9(11)
O6	0.8841(32)	0.7497(23)	-0.1560(45)	0.3506(53)	37.9(11)
O7	0.9007(23)	0.8301(18)	0.0087(40)	0.3506(53)	37.9(11)

Atomic Coordinates for MFM-300(V)-750mbarCO_2

Site	*x*	*y*	*z*	Occupancy	B_{iso} (Å^2)
V	0.691700(50)	0.308300(50)	0.5	1	3.594(26)
O1	0.74484(22)	0.25	0.625	1	3.569(41)
O2	0.89838(15)	0.28970(14)	0.99408(24)	1	3.569(41)

O3	0.61952(17)	0.38196(16)	0.39128(17)	1	3.569(41)
C1	0.59118(29)	0.35994(25)	0.70153(32)	1	4.702(61)
C2	0.54461(26)	0.43393(27)	0.76011(42)	1	4.702(61)
C3	0.5	0.5	0.70346(43)	1	4.702(61)
C4	0.54733(30)	0.43311(28)	0.87925(28)	1	4.702(61)
C5	0.5	0.5	0.93621(33)	1	4.702(61)
H3	0.5	0.5	0.6261(32)	1	5.642(73)
H4	0.57318	0.38162	0.90735	1	5.642(73)
H1	0.806	0.25	0.625	1	5.642(73)
C6	0.2402(16)	0.0376(17)	0.3098(17)	0.4575(48)	18.91(51)
O4	0.25603(82)	0.96293(56)	0.3164(10)	0.4575(48)	18.91(51)
O5	0.22427(92)	0.1122(12)	0.3032(15)	0.4575(48)	18.91(51)
C7	0.2082(40)	0.1067(41)	0.0726(28)	0.3885(45)	32.83(85)
O6	0.2476(17)	0.1259(22)	0.1512(33)	0.3885(45)	32.83(85)
O7	0.1687(13)	0.0875(17)	0.9940(29)	0.3885(45)	32.83(85)

Atomic Coordinates for MFM-300(V)-1000mbarCO_2

Site	*x*	*y*	*z*	Occupancy	B_{iso} (Å^2)
V	0.69216(5)	0.30784(5)	0.5	1	2.89(3)
O1	0.7459(2)	0.25	0.625	1	2.73(4)
O2	0.89899(16)	0.29063(15)	0.9925(3)	1	2.73(4)
O3	0.61992(18)	0.38223(18)	0.39092(18)	1	2.73(4)
C1	0.5922(3)	0.3602(3)	0.7003(3)	1	3.86(6)
C2	0.5434(3)	0.4332(3)	0.7601(4)	1	3.86(6)
C3	0.5	0.5	0.7033(5)	1	3.86(6)
C4	0.5476(3)	0.4332(3)	0.8794(3)	1	3.86(6)
C5	0.5	0.5	0.9362(4)	1	3.86(6)
H3	0.5	0.5	0.626(3)	1	4.63(8)
H4	0.57318	0.38162	0.90735	1	4.63(8)
H1	0.806	0.25	0.625	1	4.63(8)
C6	0.760(2)	0.538(2)	0.937(2)	0.477(6)	21.5(7)
O4	0.7415(10)	0.4625(7)	0.9302(13)	0.477(6)	21.5(7)
O5	0.7793(11)	0.6127(13)	0.954(2)	0.477(6)	21.5(7)
C7	0.207(4)	0.100(4)	0.075(3)	0.453(5)	32.9(9)
O6	0.2484(17)	0.121(2)	0.154(4)	0.453(5)	32.9(9)
O7	0.1672(13)	0.0956(16)	0.992(3)	0.453(5)	32.9(9)

6. Synthesis of PIM-1

To a dry 100 mL round bottom flask equipped with a Dean−Stark trap and mechanical stirrer, 5,5′,6,6′-tetrahydroxy-3,3,3′,3′-tetramethyl-1,1′-spirobisindane (3.404 g, 0.01 mol), dicyanotetrafluorobenzene (2.001 g, 0.01 mol), anhydrous K_2CO_3 (4.146 g, 0.03 mol), DMAc (20 mL) and toluene (10 mL) were added under N_2. The reaction was heated to 165 °C and carried out for 35 min (15 min used to obtain equilibrium) under reflux. The resultant highly viscous solution was immediately poured into MeOH (500 mL) in order to quench the reaction. The product was then dissolved in $CHCl_3$ (150 mL) and re-precipitated from MeOH (1 L). The product was refluxed for 18 h in deionized water, filtered and washed with acetone and then dried at 120 °C for 2 days. This gave the desired PIM-1 product (3.84 g, 83% yield). GPC (in chloroform): M_w = 230039 g mol^{-1}, and M_w/M_n = 6.001. ^{1}H NMR (500 MHz, $CDCl_3$, δ, ppm): 6.81 (2H, s), 6.43 (2H, s), 2.33−2.17 (4H, dd), 1.37−1.31 (broad, 12H). Anal. Calc. for C29H20N2O4 (wt %): C, 75.64; H, 4.37; N, 6.08. Found: C, 74.12; H, 4.24; N, 6.13.

7. PXRD of mixed matrix membrane MFM-300(VIII)/PIM-1

PXRD analysis of the membrane was conducted on a Philips X'Pert XRD using Cu Kα radiation to ensure retention of structure and crystallinity of the MOF once incorporated into the MMM.

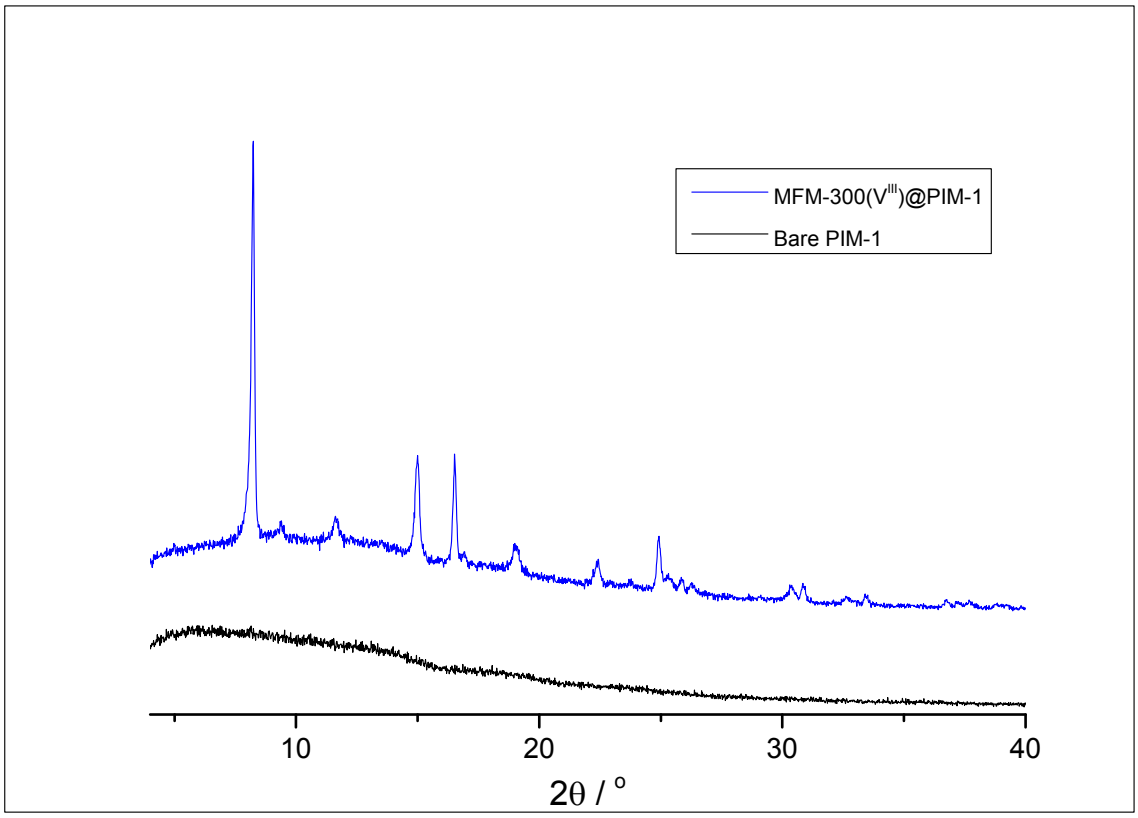

Figure S15. PXRD for PIM-1 and for MFM-300(V^{III})/PIM-1.

8. SEM of mixed matrix membrane MFM-300(VIII)/PIM-1

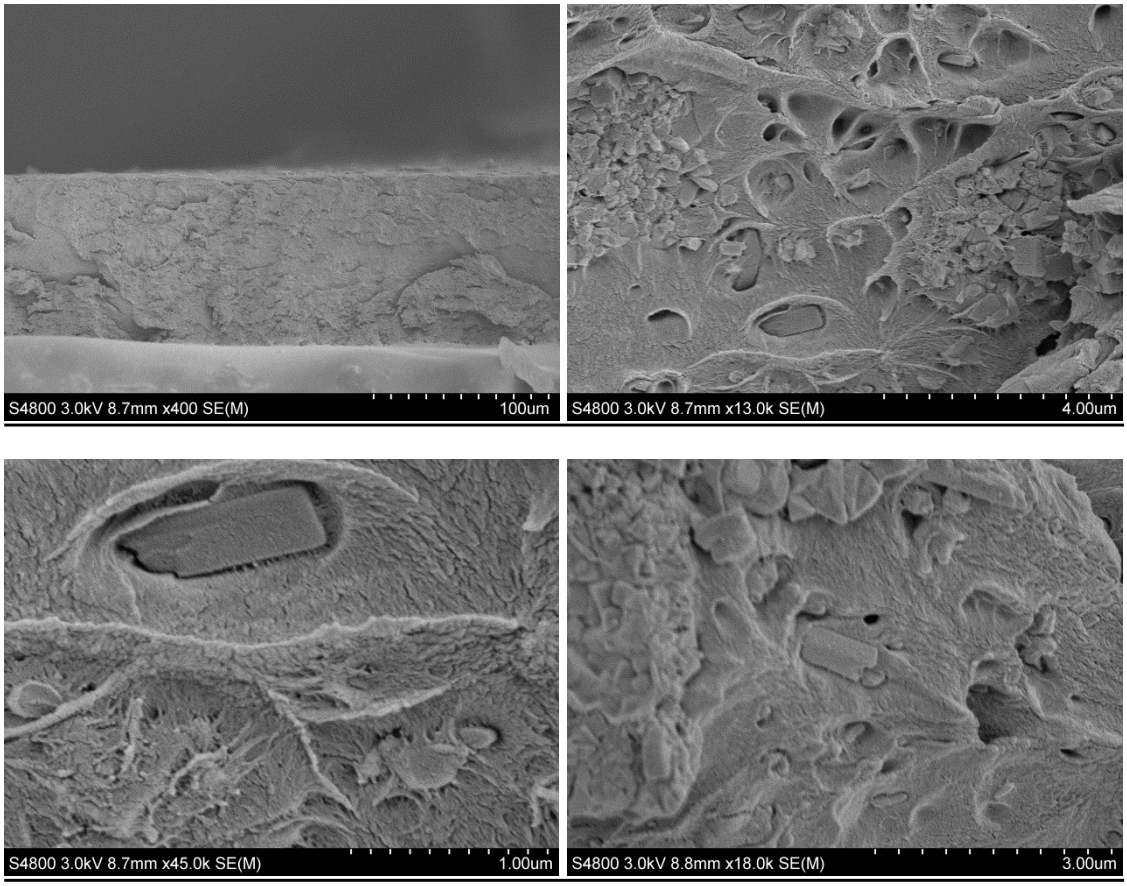

Figure S16. SEM images of the membrane cross-section showing good distribution of the MOF particles and good affinity between the particles and the polymer matrix.

9. Results of Permeation experiments

Table S3. Single gas permeation data of MFM-300(V^{III})/PIM-1 MMM.

Gas	Temperature (°C)	Solubility coefficient (cm^3(STP) cm^2 atm^{-1})	Diffusion coefficient (x10^8 cm^2 s^{-1})	Permeability coefficient (Barrer)
He	14	0.15 ± 0.01	6997 ± 451	1041 ± 2.45
	30	0.134 ± 0.008	8364 ± 562	1117 ± 1.35
	45	0.12 ± 0.0078	9819 ± 595	1191 ± 2.04
	61	0.11 ± 0.016	11816 ± 1720	1270 ± 3.90
	75	0.08 ± 0.008	16830 ± 1743	1379 ± 0.69
H_2	14	0.56 ± 0.012	4190 ± 167	2342 ± 43
	30	0.458 ± 0.013	5381 ± 141	2465 ± 4.67
	45	0.40 ± 0.015	6414 ± 229	2542 ± 2.04
	61	0.33 ± 0.022	7894 ± 492	2611 ± 6.25
	75	0.26 ± 0.017	10697 ± 668	2758 ± 4.54
N_2	14	2.0009 ± 0.057	79.38 ± 2.24	158.73 ± 1.94
	30	1.946 ± 0.008	111.39 ± 0.43	216.74 ± 0.52
	45	1.73 ± 0.012	158.14 ± 0.92	273.17 ± 1.12
	61	1.51 ± 0.006	216.98 ± 1.18	326.97 ± 1.99

	75	1.33 ± 0.017	297.84 ± 2.46	403.33 ± 1.633
CO_2	14	58.58 ± 3.51	76.09 ± 3.13	4450 ± 83.84
	30	43.032 ± 1.57	107.37 ± 2.40	4617 ± 65.56
	45	31.22 ± 1.27	146.73 ± 3.80	4578 ± 67.69
	61	22.48 ± 0.54	196.84 ± 2.77	4423 ± 45.39
	75	16.92 ± 0.26	258.66 ± 1.82	4377 ± 37.05
CH_4	14	5.72 ± 0.30	34.36 ± 1.38	196.26 ± 2.65
	30	5.84 ± 0.07	51.53 ± 0.73	301.03 ± 0.41
	45	5.26 ± 0.065	79.15 ± 0.73	415.99 ± 1.30
	61	4.58 ± 0.068	117.87 ± 1.12	539.54 ± 2.99
	75	3.89 ± 0.041	175.98 ± 2.30	683.80 ± 2.09